tvst

Article

# The Utility of Corneal Nerve Fractal Dimension Analysis in Peripheral Neuropathies of Different Etiology

**Ioannis N. Petropoulos[1], Abdulrahman Al-Mohammedi[1], Xin Chen[2], Maryam Ferdousi[3], Georgios Ponirakis[1], Harriet Kemp[4], Reena Chopra[5], Scott Hau[5], Marc Schargus[6], Jan Vollert[4,7], Dietrich Sturm[8], Tina Bharani[1], Christopher Kleinschnitz[9], Mark Stettner[9], Tunde Peto[10], Christoph Maier[11], Andrew S. C. Rice[4], and Rayaz A. Malik[1]**

[1] Division of Research, Weill Cornell Medicine–Qatar, Doha, Qatar
[2] School of Computer Science, University of Nottingham, Nottingham, UK
[3] Institute of Cardiovascular Science, University of Manchester, Manchester, UK
[4] Pain Research, Department of Surgery and Cancer, Faculty of Medicine, Imperial College London, London, UK
[5] NIHR Moorfields Clinical Research Facility, Moorfields Eye Hospital, London, UK
[6] Department of Ophthalmology, University Eye Hospital, Dusseldorf, Germany
[7] Division of Neurophysiology, Center of Biomedicine and Medical Technology Mannheim (CBTM), Medical Faculty Mannheim, Ruprecht-Karls University, Heidelberg, Germany
[8] BG Universitätsklinikum Bergmannsheil GmbH, Department of Neurology, Ruhr University, Bochum, Germany
[9] Department of Neurology, Essen University Hospital, Essen, Germany
[10] Queen's University Belfast, Belfast, Northern Ireland
[11] BG Universitätsklinikum Bergmannsheil GmbH, Department of Pain Medicine, Ruhr University, Bochum, Germany

**Correspondence:** Rayaz A. Malik, Weill Cornell Medicine–Qatar, Qatar Foundation, P.O. Box 24144, Education City, Doha, Qatar. e-mail: ram2045@qatar-med.cornell.edu

**Received:** January 23, 2020
**Accepted:** August 10, 2020
**Published:** August 28, 2020

**Keywords:** peripheral neuropathy; corneal confocal microscopy; fractals

**Citation:** Petropoulos IN, Al-Mohammedi A, Chen X, Ferdousi M, Ponirakis G, Kemp H, Chopra R, Hau S, Schargus M, Vollert J, Sturm D, Bharani T, Kleinschnitz C, Stettner M, Peto T, Maier C, Rice ASC, Malik RA. The utility of corneal nerve fractal dimension analysis in peripheral neuropathies of different etiology. Trans Vis Sci Tech. 2020;9(9):43, https://doi.org/10.1167/tvst.9.9.43

**Purpose:** Quantification of corneal confocal microscopy (CCM) images has shown a significant reduction in corneal nerve fiber length (CNFL) in a range of peripheral neuropathies. We assessed whether corneal nerve fractal dimension (CNFrD) analysis, a novel metric to quantify the topological complexity of corneal subbasal nerves, can differentiate peripheral neuropathies of different etiology.

**Methods:** Ninety patients with peripheral neuropathy, including 29 with diabetic peripheral neuropathy (DPN), 34 with chronic inflammatory demyelinating polyneuropathy (CIDP), 13 with chemotherapy-induced peripheral neuropathy (CIPN), 14 with human immunodeficiency virus-associated sensory neuropathy (HIV-SN), and 20 healthy controls (HCs), underwent CCM for estimation of corneal nerve fiber density (CNFD), CNFL, corneal nerve branch density (CNBD), CNFrD, and CNFrD adjusted for CNFL (ACNFrD).

**Results:** In patients with DPN, CIDP, CIPN, or HIV-SN compared to HCs, CNFD ($P$ = 0.004–0.0001) and CNFL ($P$ = 0.05–0.0001) were significantly lower, with a further significant reduction among subgroups. CNFrD was significantly lower in patients with CIDP compared to HCs and patients with HIV-SN ($P$ = 0.02–0.0009) and in patients with DPN compared to HCs and patients with HIV-SN, CIPN, or CIDP ($P$ = 0.001–0.0001). ACNFrD was lower in patients with CIPN, CIDP, or DPN compared to HCs ($P$ = 0.03–0.0001) and in patients with DPN compared to those with HIV-SN, CIPN, or CIDP ($P$ = 0.01–0.005).

**Conclusions:** CNFrD can detect a distinct pattern of corneal nerve loss in patients with DPN or CIDP compared to those with CIPN or HIV-SN and controls.

**Translational Relevance:** Various peripheral neuropathies are characterized by a comparable degree of corneal nerve loss. Assessment of corneal nerve topology by CNFrD could be useful in differentiating neuropathies based on the pattern of loss.

## Introduction

The prevalence, severity, and disability associated with different peripheral neuropathies vary by etiology and can pose a significant diagnostic and therapeutic challenge. The diagnosis of peripheral neuropathies has traditionally relied on identifying typical symptoms, neurological deficits with more detailed assessment using neurophysiology, quantitative sensory testing, autonomic function testing, and, if necessary, a nerve or skin biopsy.[1] CCM is a non-invasive ophthalmic imaging device which has been used to show reduced corneal subbasal nerves in DPN,[2,3] to evaluate the severity of diabetic neuropathy,[4–7] and to predict incident neuropathy.[8,9] Furthermore, CCM has been used to show significant improvement in corneal nerve morphology in several intervention studies.[10–15]

More recently, CCM has been used to investigate other peripheral neuropathies.[16–22] Stettner et al.[16] reported corneal nerve loss and increased immune cell infiltrates in patients with chronic inflammatory demyelinating polyneuropathy (CIDP). Kemp et al.[17] reported a reduction in corneal nerve density and increased tortuosity in patients with human immunodeficiency virus-associated sensory neuropathy (HIV-SN). Ferdousi et al.[18] found a decrease in the corneal nerve fiber length (CNFL) of patients with gastroesophageal cancer and an increase in patients with chemotherapy-induced peripheral neuropathy (CIPN). Corneal nerve loss has been demonstrated in a cohort of patients with transthyretin familial amyloid neuropathy[23] that was related to the severity of somatic and autonomic neuropathy, but most importantly the nerve loss could be quantified in all of the patients, avoiding the floor effect seen with sural nerve action potential and intra-epidermal nerve fiber density. More recently, we have identified corneal nerve loss in patients with Fabry disease,[24] Friedreich's ataxia,[19] and sarcoidosis[25] and have found significant correlations with neurological disability.

Given that corneal nerve loss occurs in such a wide range of peripheral neuropathies, this raises a question regarding the clinical utility of CCM for differentiating neuropathies of differing etiology. In a study of patients with type 1 diabetes, in addition to the established measures of corneal nerve morphology we have shown that corneal nerve fractal dimension (CNFrD) may allow the identification of those with DPN.[26] Fractal dimension[27] is a quantitative estimate of the topological complexity of an image feature and has been employed to describe structural alterations in the brain of patients with neurodegenerative,[28,29] neurodevelopmental,[30] and psychiatric disorders.[31] Fractal analysis allows an assessment of the topology of the main nerve fiber and branches, which, we propose, may differ according to the etiology of peripheral neuropathy. In this study, we applied fractal dimension analysis of corneal subbasal nerves in patients with metabolic (DPN), inflammatory (CIDP), toxic (CIPN), and infectious (HIV-SN) peripheral neuropathies.

## Methods

### Study Subjects

CCM images from 29 subjects with type 1 diabetes mellitus and DPN (58.5 ± 12 years old), 34 patients with CIDP (59.2 ± 14.8 years old), 13 patients with CIPN (63.8 ± 10 years old), 14 patients with HIV-SN (57.7 ± 7.8 years old), and 20 age-matched healthy controls (HCs) (58.5 ± 12 years old) were used in this study. The data presented here constitute a secondary analysis of already published data,[16–18,26] but this study utilized only the data for patients with clinically diagnosed peripheral neuropathy. This study adhered to the Tenets of the declaration of Helsinki, and ethical approval was obtained by all participating institutions. Informed written consent was obtained from all subjects prior to participation. Exclusion criteria were any cause of neuropathy other than the primary cause of neuropathy (deficiency of vitamin $B_{12}$ or folate; autoimmune infectious; rheumatological disease) or having corneal dystrophies, active anterior eye infections, using contact lens on a regular basis, or having had recent (<1 year) refractive or cataract surgery.

### Corneal Confocal Microscopy

All study participants underwent CCM with a Heidelberg Retinal Tomograph III Rostock Cornea Module (Heidelberg Engineering, Heidelberg, Germany). This device uses a 670-nm wavelength helium neon diode laser, which is a class I laser and therefore does not pose any ocular safety hazard. A 63× objective lens with a numerical aperture of 0.9 and a working distance, relative to the applanating cap (TomoCap, Heidelberg Engineering), of 0.0 to 3.0 mm was used. The size of each two-dimensional image produced was 384 × 384 pixels, corresponding to 400 µm × 400 µm and equivalent to 1.04 µm/pixel. To perform the CCM examination, local anesthetic (0.4% benoxinate hydrochloride; Chauvin Pharmaceuticals, Chefaro, UK) was used to anesthetize each eye, and Viscotears (carbomer 980, 0.2%; Novartis UK, London, UK) was used as the coupling agent between

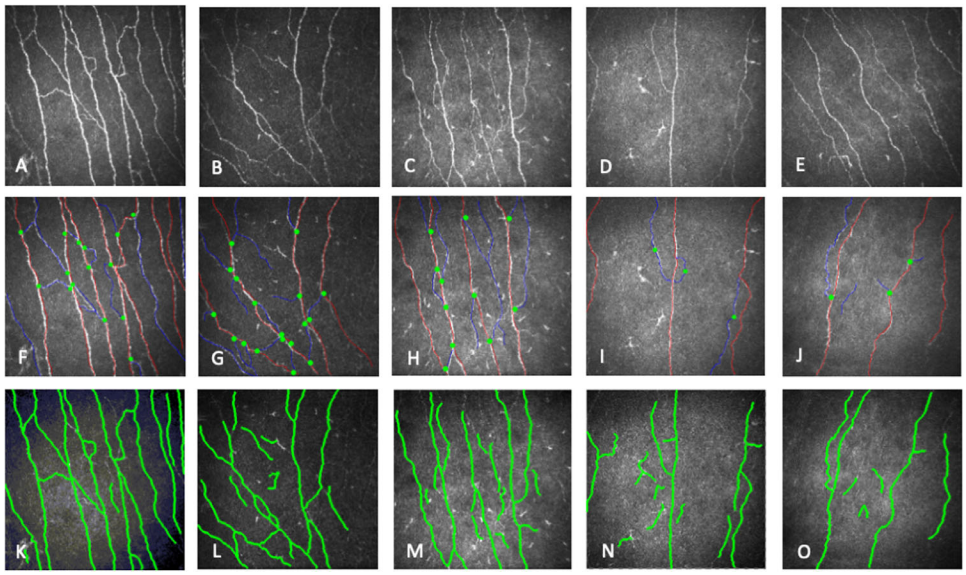


**Figure 1.** (*Top row*) Original CCM images from a HC (A) and from patients with HIV-SN (B), CIPN (C), CIDP (D), and DPN (E). (*Middle row*) Corresponding images analyzed with CCMetrics for estimation of CNFD (*red*), CNBD (*green dots*), and CNFL (*red* and *blue*) in HCs (F) and in patients with HIV-SN (G), CIPN (H), CIDP (I), or DPN (J). (*Bottom row*) Images analyzed for estimation of the novel metric CNFrD in HCs (CNFrD = 1.55) (K), HIV-SN (CNFrD = 1.5) (L), CIPN (CNFrD = 1.51) (M), CIDP (CNFrD = 1.45) (N), and DPN (CNFrD = 1.41) (O). Although CNFD and CNFL were significantly reduced in groups of patients compared to HCs, the underlying morphology assessed by CNFrD also appears significantly altered compared to HCs and among groups of patients.

the cornea and the applanating cap. All subjects were asked to fixate on an outer fixation light throughout the CCM scan, and an external CCD camera was used to position the applanating cap correctly onto the central cornea. Images were acquired using the "section" mode in the Heidelberg Eye Explorer software. Based on depth, contrast, and focus position, six images per subject (three per eye) from the central subbasal nerve plexus were selected for analysis. CCM image examples from a HC and from participants with HIV, CIPN, CIDP, and T1DM are presented in Figures 1A to 1E.

## Image Analysis

In total, 660 CCM images from both eyes were analyzed independently using manual semiautomated, purpose-designed CCM image segmentation software (CCMetrics; M.A. Dabbah, X. Chen, J. Graham, and R.A. Malik, University of Manchester, Manchester, UK) (Figs. 1F–1J) and the automated version (ACCMetrics).[32] CCMetrics is a validated CCM image segmentation algorithm that allows measurement of corneal nerve fiber density (CNFD) (fibers/mm$^2$), the number of main nerve fibers per image divided by the area of the image; corneal nerve branch density (CNBD) (branches/mm$^2$), the number of main nerve branches; CNFL (mm/mm$^2$), the sum of the length of all nerves per image (main nerves and branches). ACCMetrics was used for the estimation of CNFrD as previously described.[26] For CNFrD estimation, all original CCM images (Fig. 2A) were resized to 512 × 512 pixels, as this was the image resolution used to train our machine learning-based nerve fiber detection mode.[32] CNFrD was calculated based on the binary image representing the detected nerve fibers using our previously developed machine learning approach,[32] as shown in Figure 2B. CNFrD measures nerve complexity as the ratio of the change in detail to the change in scale in a CCM image. Box counting is a widely used and acknowledged method for fractal analysis calculation,[33] and it was applied in our study. This technique uses various sizes of $n \times n$ boxes (in our study, $n = 1, 2, 4, \ldots, 512$, as 512 was the image width) to split the image into small patches. For each of the box sizes, the total number of boxes, $Y_i$ ($i$ is the index of the different box sizes), that contain nerve fibers are recorded. As shown in Figure 2C, the logarithm of $Y$ against the logarithm of $n$ is then plotted. A first-order polynomial (i.e., red line in Fig. 2C) is fitted to these points using the method of least squares, where the coefficient of the line fitting (i.e., slope of the line, denoted as $C$) is calculated. Subsequently, $-C$ is used as the fractal dimension value of a given CCM image (i.e., CNFrD). The CNFrD value is unitless, as it is a ratio, and increases when the number of counted small boxes increases, indicating a more complicated structure (e.g., higher CNFrD in a

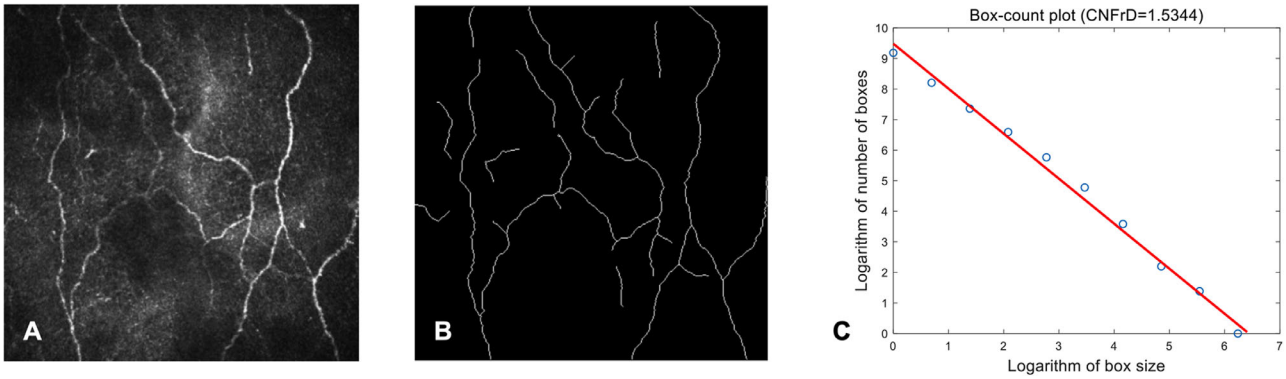


**Figure 2.** (A) Original CMM image, (B) detected nerve fibers using a machine learning method,[32] and (C) CNFrD calculation using the box counting method.

healthy control subject). In contrast, fewer, shorter, or disrupted nerve fibers result in a lower CNFrD value that reflects altered morphology (Figs. 1K–1O). To adjust for the severity of corneal nerve fiber loss, a ratio of CNFL/CNFrD was calculated (CNFrD adjusted for CNFL, or ACNFrD), which is also unitless. The averaged result of six images per patient was used for CNFD, CNBD, CNFL, CNFrD, and ACNFrD.

### Statistical Analysis

GraphPad Prism 8 (GraphPad Software, San Diego, CA) was used for the statistical analysis and graphic illustrations. A Shapiro–Wilk test was used to assess data for normality ($P < 0.05$). Data were confirmed to follow a normal distribution, and one-way analysis of variance (post hoc Bonferroni–Sidak test) was used to compare the results among participant groups and controls, respectively. All data are expressed as mean ± standard deviation, and a $P < 0.05$ was considered statistically significant.

## Results

### Demographics

There was no significant difference in age among the different groups of patients except for patients with CIPN, who were slightly older ($P = 0.06$) compared to HCs (Table 1). Patients with HIV-SN (14 males, 0 females), CIPN (19 males, 1 female), or CIDP (22 males, 12 females) were predominantly male compared to those having DPN (12 males, 17 females), for whom there was a slightly higher prevalence among females. Glycated hemoglobin (HbA1c) was within normal range, indicating no diabetes for HCs (38 ± 3.8 mmol/mol) or for patients with HIV-SN (within normal range), CIPN (34.8 ± 5.8 mmol/mol), or CIDP (35.9 ± 6.8). HbA1c was high for patients with DPN indicating diabetes (72.4 ± 19.3 mmol/mol). Disease duration was longer for HIV-SN (25.3 ± 4.7 years), CIDP (12 ± 8.6 years), and DPN (42 ± 14.4 years) but shorter for CIPN (<6 months), as expected.

### Corneal Confocal Microscopy

The detailed results are presented in Table 1 and Figure 3. CNFD was significantly lower in patients with HIV-SN ($P < 0.0001$), CIPN ($P = 0.004$), CIDP ($P < 0.0001$), or DPN ($P < 0.0001$) compared to HCs and was lower in DPN compared to HIV-SN ($P = 0.002$), CIPN ($P < 0.0001$), or CIDP ($P = 0.001$) (Fig. 3A). CNBD was significantly lower only in DPN compared to HCs ($P < 0.0001$) or CIDP ($P = 0.003$) (Fig. 3B). CNFL was significantly lower in patients with CIPN ($P = 0.05$), CIDP ($P = 0.0001$), or DPN ($P < 0.0001$) compared to HCs and was lower in DPN compared to HIV-SN ($P = 0.002$), CIPN ($P = 0.01$), or CIDP ($P = 0.02$) (Fig. 3C). CNFrD was significantly lower in patients with CIDP compared to HCs ($P = 0.0009$) or HIV-SN ($P = 0.02$) and in DPN compared to HCs ($P < 0.0001$), HIV-SN ($P < 0.0001$), CIPN ($P < 0.0001$), or CIDP ($P = 0.001$) (Fig. 3D). ACNFrD was lower in patients with CIPN ($P = 0.03$), CIDP ($P = 0.0007$), or DPN ($P < 0.0001$) compared to HCs and differed in DPN compared to HIV-SN ($P = 0.005$), CIPN ($P = 0.01$), or CIDP ($P = 0.01$) (Fig. 3E).

## Discussion

To the best of our knowledge, this is the first study to compare established measures of corneal

**Table.** Demographic and CCM Parameter Results

| | Mean | SD | HC ($n = 20$) | HIV-SN ($n = 14$) | CIPN ($n = 34$) | CIDP ($n = 29$) |
|---|---|---|---|---|---|---|
| Age (y) | | | | | | |
| HC | 54.5 | 11.2 | | | | |
| HIV-SN | 57.7 | 7.8 | 0.99 | | | |
| CIPN | 63.8 | 10.0 | 0.06 | — | | |
| CIDP | 59.2 | 14.8 | 0.52 | — | — | |
| DPN | 58.5 | 12.0 | 0.71 | — | — | — |
| CNFD (fibers/mm$^2$) | | | | | | |
| HC | 39.4 | 6.7 | | | | |
| HIV-SN | 26.7 | 4.2 | <0.0001 | | | |
| CIPN | 29.5 | 5.5 | 0.004 | 0.99 | | |
| CIDP | 25.1 | 7.7 | <0.0001 | 0.79 | 0.55 | |
| DPN | 17.4 | 9.9 | <0.0001 | 0.002 | <0.0001 | 0.001 |
| CNBD (branches/mm$^2$) | | | | | | |
| HC | 95.9 | 40.2 | | | | |
| HIV-SN | 74.0 | 22.0 | 0.6 | | | |
| CIPN | 73.6 | 43.3 | 0.61 | 0.99 | | |
| CIDP | 80.3 | 40.2 | 0.77 | 0.99 | 0.99 | |
| DPN | 45.7 | 31.7 | <0.0001 | 0.18 | 0.22 | 0.003 |
| CNFL (mm/mm$^2$) | | | | | | |
| HC | 27.3 | 4.7 | | | | |
| HIV-SN | 22.2 | 3.4 | 0.16 | | | |
| CIPN | 21.3 | 5.0 | 0.05 | 0.99 | | |
| CIDP | 19.4 | 6.0 | 0.0001 | 0.8 | 0.98 | |
| DPN | 14.6 | 8.2 | <0.0001 | 0.002 | 0.0133 | 0.02 |
| CNFrD (unitless) | | | | | | |
| HC | 1.51 | 0.02 | | | | |
| HIV-SN | 1.51 | 0.02 | 0.99 | | | |
| CIPN | 1.50 | 0.03 | 0.99 | 0.99 | | |
| CIDP | 1.46 | 0.04 | 0.0009 | 0.02 | 0.12 | |
| DPN | 1.40 | 0.08 | <0.0001 | <0.0001 | <0.0001 | 0.001 |
| ACNFrD (unitless) | | | | | | |
| HC | 18.0 | 3.0 | | | | |
| HIV-SN | 14.7 | 2.2 | 0.07 | | | |
| CIPN | 14.2 | 3.1 | 0.03 | 0.79 | | |
| CIDP | 13.4 | 4.0 | 0.0007 | 0.67 | 0.78 | |
| DPN | 10.2 | 5.3 | <0.0001 | 0.005 | 0.01 | 0.01 |

$P < 0.05$ was considered significant.

nerve loss and CNFrD[26] in peripheral neuropathies of differing etiology. There are two main findings in this study. First, patients with DPN or CIDP showed more severe corneal nerve loss compared to patients with HIV-SN or CIPN, who had milder albeit significant loss. Our second and most important finding is that the remaining corneal nerves may have a distinct morphological pattern, as assessed by CNFrD in DPN and CIDP compared to HIV-SN and CIPN. Furthermore, even after adjustment for the overall severity of reduction in CNFL, ACNFrD differed significantly in patients with DPN compared to CIDP, HIV-SN, and CIPN.

Peripheral neuropathy occurs in the setting of many common and rare neurologic disorders. It affects approximately 26% to 58% of patients with diabetes,[34,35] up to 50% of people living with HIV,[36] and 68% of patients with cancer after chemotherapy.[37] CIDP affects 5 out of 100,000 people.[38,39] The corneal subbasal nerve plexus is a dense network of

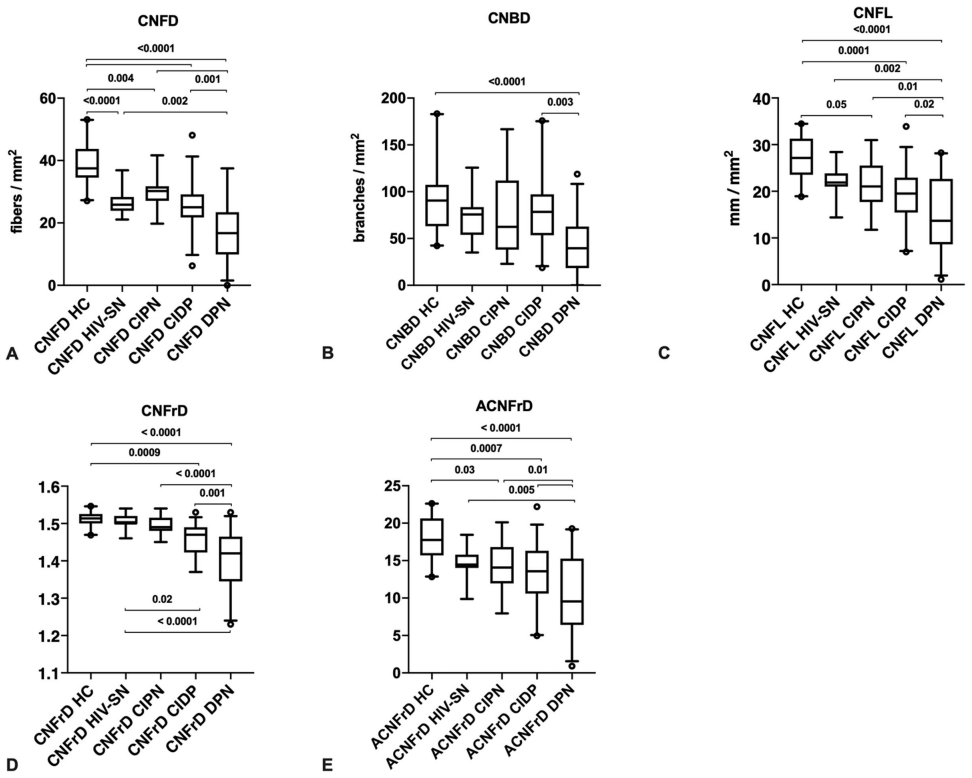


**Figure 3.** Box and whisker plots of corneal nerve morphology parameters in controls and neuropathy groups. The box represents the mean (*solid line*) with 25th and 75th percentiles; whiskers represent 5th and 95th percentiles for CNFD (A), CNBD (B), CNFL (C), CNFrD (D), and the CNFL/CNFrD ratio (ACNFrD) (E), with *black circles* representing outliers in the sample. One-way analysis of variance was used to compare between groups.

unmyelinated C-fibers, which are anatomically similar to intra-epidermal nerve fibers,[40,41] the gold standard markers for assessing small fiber integrity. Unlike intra-epidermal innervation, which requires an invasive skin biopsy, corneal subbasal innervation can be quantified rapidly and non-invasively using in vivo CCM. We have previously shown that corneal nerve loss occurs in DPN,[2–9] CIDP,[16] HIV-SN,[17] and CIPN.[18] More recently, we and others have also shown corneal nerve loss in patients with Parkinson's disease,[42] multiple sclerosis,[43–45] and dementia.[46] These findings highlight the potential of CCM as a surrogate measure of neurodegeneration but also raise concerns regarding the clinical utility of this technique due to limited specificity.

Fractal dimension analysis is a measure of tissue structural complexity, and in brain magnetic resonance imaging scans[28–31] it has been used to identify distinct tissue geometric patterns in different neurodegenerative diseases. In ophthalmology research, fractal dimension analysis has been used to study alterations in the retinal vascular network in diabetic retinopathy[47] and maculopathy[48] and to detect glaucoma in digital images.[49,50] A recent study has used spatial analysis to show increased clustering of corneal nerve loss in patients with early diabetic neuropathy[51] and we have shown altered CNFrD in patients with DPN.[26] In this context, our findings suggest that in addition to demonstrating corneal nerve loss, there may be specific imaging traits of remaining nerve fibers associated with the underlying etiology.

Strengths of this study are the detailed clinical phenotyping of neuropathy and the homogeneous imaging protocol used between centers. Given that ex vivo[41] and in vivo CCM studies[52,53] have shown that nerves in the inferior cornea are highly tortuous with a whorl-like appearance compared to almost straight nerves in the central cornea, all measurements were performed from the central cornea using a standardized protocol. A main limitation is the use of an automated image analysis algorithm to estimate CNFrD. Because CNFrD depends on accurate nerve segmentation, it may have been underestimated compared to the true fractal dimension.[4] Another limitation is the relatively small sample size, particularly for people living with HIV and CIPN, which may have skewed the results toward milder neuropathy. Finally, as only images from the central region were quantified for CNFrD, we cannot exclude the possibility of image selection bias.

Assessment of wide-field CCM images may provide additional value for the estimation of CNFrD. Nevertheless, we show that fractal dimension analysis could complement the existing toolbox of corneal nerve analysis metrics and help to differentiate peripheral neuropathies, especially CIDP and DPN. We believe the additional quantification of CNFrD enhances the clinical utility of CCM by enhancing the specificity of this technique. Future studies should assess whether corneal nerve fractal dimension can differentiate central from peripheral neurodegenerative disorders.

## Acknowledgments

Supported by a grant from the Qatar National Research Fund (BMRP 20038654) and by an Innovative Medicines Initiative Joint Undertaking grant agreement (115007), resources for which are composed of financial contributions from the European Union's Seventh Framework Program (FP7/2007-2013) and in-kind contributions from the European Federation of Pharmaceutical Industries and Associations companies. H.K. was also supported by Neuropain (European Union's Seventh Framework Programme grant HEALTH F2-2013-602891).

Disclosure: **I.N. Petropoulos**, None; **A. Al-Mohammedi**, None; **X. Chen**, None; **M. Ferdousi**, None; **G. Ponirakis**, None; **H. Kemp**, None; **R. Chopra**, None; **S. Hau**, None; **M. Schargus**, None; **J. Vollert**, None; **D. Sturm**, None; **T. Bharani**, None; **C. Kleinschnitz**, None; **M. Stettner**, None; **T. Peto**, None; **C. Maier**, None; **A.S.C. Rice**, None; **R.A. Malik**, None

## References

1. Gwathmey KG, Pearson KT. Diagnosis and management of sensory polyneuropathy. *BMJ*. 2019;365:l1108.
2. Malik RA, Kallinikos P, Abbott C, et al. Corneal confocal microscopy: a non-invasive surrogate of nerve fibre damage and repair in diabetic patients. *Diabetologia*. 2003;46:683–688.
3. Asghar O, Petropoulos IN, Alam U, et al. Corneal confocal microscopy detects neuropathy in subjects with impaired glucose tolerance. *Diabetes Care*. 2014;37:2643–2646.
4. Petropoulos IN, Alam U, Fadavi H, et al. Rapid automated diagnosis of diabetic peripheral neuropathy with in vivo corneal confocal microscopy. *Invest Ophthalmol Vis Sci*. 2014;55:2071–2078.
5. Tavakoli M, Quattrini C, Abbott C, et al. Corneal confocal microscopy: a novel noninvasive test to diagnose and stratify the severity of human diabetic neuropathy. *Diabetes Care*. 2010;33:1792–1797.
6. Ahmed A, Bril V, Orszag A, et al. Detection of diabetic sensorimotor polyneuropathy by corneal confocal microscopy in type 1 diabetes: a concurrent validity study. *Diabetes Care*. 2012;35:821–828.
7. Perkins BA, Lovblom LE, Bril V, et al. Corneal confocal microscopy for identification of diabetic sensorimotor polyneuropathy: a pooled multinational consortium study. *Diabetologia*. 2018;61:1856–1861.
8. Azmi S, Ferdousi M, Petropoulos IN, et al. Corneal confocal microscopy identifies small-fiber neuropathy in subjects with impaired glucose tolerance who develop type 2 diabetes. *Diabetes Care*. 2015;38:1502–1508.
9. Pritchard N, Edwards K, Russell AW, Perkins BA, Malik RA, Efron N. Corneal confocal microscopy predicts 4-year incident peripheral neuropathy in type 1 diabetes. *Diabetes Care*. 2015;38:671–675.
10. Mehra S, Tavakoli M, Kallinikos PA, et al. Corneal confocal microscopy detects early nerve regeneration after pancreas transplantation in patients with type 1 diabetes. *Diabetes Care*. 2007;30:2608–2612.
11. Tavakoli M, Mitu-Pretorian M, Petropoulos IN, et al. Corneal confocal microscopy detects early nerve regeneration in diabetic neuropathy after simultaneous pancreas and kidney transplantation. *Diabetes*. 2013;62:254–260.
12. Culver DA, Dahan A, Bajorunas D, et al. Cibinetide improves corneal nerve fiber abundance in patients with sarcoidosis-associated small nerve fiber loss and neuropathic pain. *Invest Ophthalmol Vis Sci*. 2017;58:BIO52–BIO60.
13. Lewis EJH, Perkins BA, Lovblom LE, Bazinet RP, Wolever TMS, Bril V. Effect of omega-3 supplementation on neuropathy in type 1 diabetes: a 12-month pilot trial. *Neurology*. 2017;88:2294–2301.
14. Brines M, Dunne AN, van Velzen M, et al. ARA 290, a nonerythropoietic peptide engineered from erythropoietin, improves metabolic control and neuropathic symptoms in patients with type 2 diabetes. *Mol Med*. 2014;20:658–666.
15. Azmi S, Jeziorska M, Ferdousi M, et al. Early nerve fibre regeneration in individuals with type 1 diabetes after simultaneous pancreas and kidney transplantation. *Diabetologia*. 2019;62:1478–1487.
16. Stettner M, Hinrichs L, Guthoff R, et al. Corneal confocal microscopy in chronic inflammatory

demyelinating polyneuropathy. *Ann Clin Transl Neurol*. 2016;3:88–100.
17. Kemp HI, Petropoulos IN, Rice AS, et al. Use of corneal confocal microscopy to evaluate small nerve fibers in patients with human immunodeficiency virus. *JAMA Ophthalmol*. 2017;135:795–800.
18. Ferdousi M, Azmi S, Petropoulos IN, et al. Corneal confocal microscopy detects small fibre neuropathy in patients with upper gastrointestinal cancer and nerve regeneration in chemotherapy induced peripheral neuropathy. *PLoS One*. 2015;10:e0139394.
19. Pagovich OE, Vo ML, Zhao ZZ, et al. Corneal confocal microscopy: neurologic disease biomarker in Friedreich ataxia. *Ann Neurol*. 2018;84:893–904.
20. Bitirgen G, Tinkir Kayitmazbatir E, Satirtav G, Malik RA, Ozkagnici A. In vivo confocal microscopic evaluation of corneal nerve fibers and dendritic cells in patients with Behçet's disease. *Front Neurol*. 2018;9:204.
21. Tavakoli M, Marshall A, Thompson L, et al. Corneal confocal microscopy: a novel noninvasive means to diagnose neuropathy in patients with Fabry disease. *Muscle Nerve*. 2009;40:976–984.
22. Rousseau A, Cauquil C, Dupas B, et al. Potential role of in vivo confocal microscopy for imaging corneal nerves in transthyretin familial amyloid polyneuropathy. *JAMA Ophthalmol*. 2016;134:983–989.
23. Rousseau A, Cauquil C, Dupas B, et al. Potential role of in vivo confocal microscopy for imaging corneal nerves in transthyretin familial amyloid polyneuropathy. *JAMA Ophthalmol*. 2016;134:983–989.
24. Bitirgen G, Turkmen K, Malik RA, Ozkagnici A, Zengin N. Corneal confocal microscopy detects corneal nerve damage and increased dendritic cells in Fabry disease. *Sci Rep*. 2018;8:12244.
25. Brines M, Culver DA, Ferdousi M, et al. Corneal nerve fiber size adds utility to the diagnosis and assessment of therapeutic response in patients with small fiber neuropathy. *Sci Rep*. 2018;8:4734.
26. Chen X, Graham J, Petropoulos IN, et al. Corneal nerve fractal dimension: a novel corneal nerve metric for the diagnosis of diabetic sensorimotor polyneuropathy. *Invest Ophthalmol Vis Sci*. 2018;59:1113–1118.
27. Mandelbrot BB. *The Fractal Geometry of Nature*. New York, NY: W.H. Freeman; 1983.
28. King RD, Brown B, Hwang M, Jeon T, George AT, Alzheimer's Disease Neuroimaging Initiative. Fractal dimension analysis of the cortical ribbon in mild Alzheimer's disease. *NeuroImage*. 2010;53:471–479.
29. Esteban FJ, Sepulcre J, de Miras JR,, *et al.* Fractal dimension analysis of grey matter in multiple sclerosis. *J Neurol Sci*. 2009;282:67–71.
30. Esteban FJ, Padilla N, Sanz-Cortés M, et al. Fractal-dimension analysis detects cerebral changes in preterm infants with and without intrauterine growth restriction. *NeuroImage*. 2010;53:1225–1232.
31. Sandu A-L, Rasmussen Jr I-A, Lundervold A, et al. Fractal dimension analysis of MR images reveals grey matter structure irregularities in schizophrenia. *Comput Med Imaging Graph*. 2008;32:150–158.
32. Chen X, Graham J, Dabbah MA, Petropoulos IN, Tavakoli M, Malik RA. An automatic tool for quantification of nerve fibers in corneal confocal microscopy images. *IEEE Trans Biomed Eng*. 2016;64:786–794.
33. Falconer K. *Fractal Geometry: Mathematical Foundations and Applications*. New York, NY: John Wiley & Sons; 2004.
34. Maser RE, Steenkiste AR, Dorman JS, et al. Epidemiological correlates of diabetic neuropathy: report from Pittsburgh Epidemiology of Diabetes Complications Study. *Diabetes*. 1989;38:1456–1461.
35. Pradeepa R, Rema M, Vignesh J, Deepa M, Deepa R, Mohan V. Prevalence and risk factors for diabetic neuropathy in an urban south Indian population: the Chennai Urban Rural Epidemiology Study (CURES-55). *Diabet Med*. 2008;25:407–412.
36. Ellis RJ, Rosario D, Clifford DB, et al. Continued high prevalence and adverse clinical impact of human immunodeficiency virus-associated sensory neuropathy in the era of combination antiretroviral therapy: the CHARTER Study. *Arch Neurol*. 2010;67:552–558.
37. Seretny M, Currie GL, Sena ES, et al. Incidence, prevalence, and predictors of chemotherapy-induced peripheral neuropathy: a systematic review and meta-analysis. *Pain*. 2014;155:2461–2470.
38. McLeod J, Pollard J, Macaskill P, Mohamed A, Spring P, Khurana V. Prevalence of chronic inflammatory demyelinating polyneuropathy in New South Wales, Australia. *Ann Neurol*. 1999;46:910–913.
39. Lunn M, Manji H, Choudhary P, Hughes R, Thomas P. Chronic inflammatory demyelinating polyradiculoneuropathy: a prevalence study in

south east England. *J Neurol Neurosurg Psychiatry*. 1999;66:677–680.
40. Quattrini C, Tavakoli M, Jeziorska M, et al. Surrogate markers of small fiber damage in human diabetic neuropathy. *Diabetes*. 2007;56:2148–2154.
41. Müller L, Pels L, Vrensen G. Ultrastructural organization of human corneal nerves. *Invest Ophthalmol Vis Sci*. 1996;37:476–488.
42. Kass-Iliyya L, Javed S, Gosal D, et al. Small fiber neuropathy in Parkinson's disease: a clinical, pathological and corneal confocal microscopy study. *Parkinsonism Relat Disord*. 2015;21:1454–1460.
43. Mikolajczak J, Zimmermann H, Kheirkhah A, et al. Patients with multiple sclerosis demonstrate reduced subbasal corneal nerve fibre density. *Mult Scler*. 2017;23:1847–1853.
44. Petropoulos IN, Kamran S, Li Y, et al. Corneal confocal microscopy: an imaging endpoint for axonal degeneration in multiple sclerosis. *Invest Ophthalmol Vis Sci*. 2017;58:3677–3681.
45. Bitirgen G, Akpinar Z, Malik RA, Ozkagnici A. Use of corneal confocal microscopy to detect corneal nerve loss and increased dendritic cells in patients with multiple sclerosis. *JAMA Ophthalmol*. 2017;135:777–782.
46. Ponirakis G, Al Hamad H, Sankaranarayanan A, et al. Association of corneal nerve fiber measures with cognitive function in dementia. *Ann Clin Transl Neurol*. 2019;6:689–697.
47. Zahid S, Dolz-Marco R, Freund KB, et al. Fractal dimensional analysis of optical coherence tomography angiography in eyes with diabetic retinopathy. *Invest Ophthalmol Vis Sci*. 2016;57:4940–4947.
48. Thomas GN, Ong S-Y, Tham YC, et al. Measurement of macular fractal dimension using a computer-assisted program. *Invest Ophthalmol Vis Sci*. 2014;55:2237–2243.
49. Wu R, Cheung CY-L, Saw SM, Mitchell P, Aung T, Wong TY. Retinal vascular geometry and glaucoma: the Singapore Malay Eye Study. *Ophthalmology*. 2013;120:77–83.
50. Lamani D, Manjunath TC, Mahesh M, Nijagunarya YS. *Retinal Nerve Fiber Layer Analysis in Digital Fundus Images: Application to Early Glaucoma Diagnosis*. New Delhi, India: Springer; 2016:69–79.
51. Ziegler D, Winter K, Strom A, et al. Spatial analysis improves the detection of early corneal nerve fiber loss in patients with recently diagnosed type 2 diabetes. *PLoS One*. 2017;12:e0173832.
52. Petropoulos IN, Ferdousi M, Marshall A, et al. The inferior whorl for detecting diabetic peripheral neuropathy using corneal confocal microscopy. *Invest Ophthalmol Vis Sci*. 2015;56:2498–2504.
53. Kalteniece A, Ferdousi M, Petropoulos I, et al. Greater corneal nerve loss at the inferior whorl is related to the presence of diabetic neuropathy and painful diabetic neuropathy. *Sci Rep*. 2018;8:3283.